Supporting Information

Chitosan cross-linked poly(aminoanthraquinone)/Prussian blue ternary nitrogen precursor-derived Fe-N-C oxygen reduction catalysts for microbial fuel cells and zinc-air battery

Guoquan Zhang,* Li Li, Mengyao Chen, Fenglin Yang

Key Laboratory of Industrial Ecology and Environmental Engineering, Ministry of Education, School of Environmental Science and Technology, Dalian University of Technology, Linggong road 2#, Dalian 116024, China.

**Corresponding Author*
E-mail: guoquanz@126.com (G. Zhang)

Contents

S1. Chemicals and reagents. 1,5-Diaminoanthraquinone (DAA), CrO_3, dimethylformamide (DMF), chitosan (low molecular weight), potassium ferricyanide(III) ($K_3Fe(CN)_6$, >99%), iron(III) chloride ($FeCl_3$, >97%), isopropanol, Nafion (5 wt%) and Pt/C E-TEK (20 wt%) were purchased from Alfar Aesar (Tianjin, China) as chemical pure reagents and used without further purification. All other chemicals were of analytical grade, and all solutions including 0.1 mol L^{-1} KOH (pH = 13.0) and 0.1 mol L^{-1} phosphate buffer solution (PBS, pH = 6.86) were prepared using Millipore Milli-Q (18.2 MΩ cm) deionized water.

S2. Preparation of chitosan cross-linked PDAA/PB precursor. Typical procedure was as follows: 5 mmol (ca. 1.2 g) 1,5-diaminoanthraquinone monomer (DAA) was first dissolved in 60 mL 1.0 mol L^{-1} H_2SO_4 nonaqueous DMF medium, and then the mixture was poured into 250 mL glass flask and stirred vigorously for 30 min in a 20 ^{0}C water bath to form **solution I.** Simultaneously, 5 mmol (ca. 1.2 g) CrO_3 was also dissolved in 10 mL 1.0 mol L^{-1} H_2SO_4 nonaqueous DMF medium containing 1.0 mol L^{-1} $FeCl_3$ to form **solution II** as oxidant. After adding 15 mg chitosan (≥ 99%) and 50 ml 50 mmol L^{-1} potassium ferrocyanide ($K_4Fe(CN)_6$) into **solution I** (the molar ratio of DAA/PB is about 2.0), the oxidant **solution II** was added dropwise at a rate of 1 drop per 3 s and the polymerization reaction mixture was stirred continuously for 48 h at 20 ^{0}C. After that, the resulting polymer precipitates were isolated from the reaction mixture by filtration and washed with DMF, ethanol and excess distilled water for several times to remove the remaining monomer, oxidant, and oligomers, followed by drying in an oven at 60 ^{0}C for 3 h. The black color implied the success polymerization

of DAA monomer and the obtained PDAA/PB polymer owning a largely π-conjugated chain structure.[1]

S3. Preparation of the modified GC electrode. Prior to use, the GC disk electrode (Φ_{GC} = 5.0 mm, geometric area: 0.196 cm^2) was polished with 1.0, 0.3, and 0.05 mm γ-Al_2O_3 powders, then rinsed with ethanol and water thoroughly in an ultrasonic bath to remove any alumina residues, and finally dried with the infrared lamp. The catalyst was transferred to GC disk by the following procedure:[2] 2 mg catalyst powder was first dispersed in 500 μL mixed solution containing 495 μL water/isopropanol solvent (ca. 79:20 v/v) and 5 μL Nafion (0.5 wt%) by 30 min sonication, reaching a homogeneous suspension with the catalyst concentration of ca. 4.0 mg mL^{-1}. Then, 15 μL catalyst inks were dropped onto the GC disk with the loading amount of 0.31 mg cm^{-2}. To prepare the Pt/C-loaded electrode, 2.0 mg catalyst was dispersed in 500 μL water/isopropanol-Nafion solution, and then 5 μL of the resulting suspension was dropped onto the GC disk with a loading amount of 0.1 mg cm^{-2} (20 μg Pt cm^{-2}).

S4. Electrochemical measurement. The GC working electrode was first subject to electrochemical polishing between 0-1.4 V before recording ORR CV curves at a scan rate of 100 mV s^{-1} for 10 min, aiming to remove the surface contaminations of the catalyst materials. Then, the CV curves were collected in the potential range of 0 to 1.1 V (vs. RHE) with a scan rate of 50 mV s^{-1} in an O_2-saturated 0.1 mol L^{-1} KOH and 0.1 mol L^{-1} PBS solutions. The LSV-RDE ORR activity was carried out in the potential range of 0.2 to 1.2 V (vs. RHE) with a scan rate of 10 mV s^{-1}, and the electrode rotating speed for LSV-RDE experiments are 400, 625, 900, 1,225, 1,600,

2,025 and 2500 rpm. Methanol tolerance of the catalysts was tested by conducting the ORR in O_2-saturated 0.1 mol L^{-1} KOH and PBS solutions by adding 8 mL 1.0 mol L^{-1} methanol. Electrochemical impedance spectroscopy (EIS, FRD100, PAR) was carried out by scanning the frequency range from 100 kHz to 10 mHz with a superimposed AC signal of 10 mV amplitude at a constant potential (E = 0.65 V) in O_2-saturated 0.1 M PBS solution. For all the ORR tests, 60 sccm (standard cubic centimeters per minute) of O_2 was bubbled into the electrolyte for 1 h prior to measurement and 30 sccm of O_2 was maintained during the test to ensure the continued O_2 saturation.

S5. The preparation of air-cathode. The air-cathode was prepared according to Feng et al.'s method,[3] which included a carbon cloth matrix, a gas diffusion layer (GDL), and a catalyst layer. The conductive GDL was made by hot-pressing carbon black slurry and polytetrafluoroethylene (PTFE) (mass ratio of 3:7) at 120 ^{0}C and 20 MPa pressure, then heated at 340 ^{0}C for 20 min. The Fe-N-C/800-HT2 catalyst layer of air-cathode was composed of the catalyst and PTFE with a mass ratio of 6:1 and was rolled on the opposite side of GDL with a catalyst loading of 2.0 mg cm^{-2}. For comparison, the Pt/C air-cathode was prepared using Pt/C E-TEK (20 wt%) with a Pt loading of 0.5 mg cm^{-2}. The projected surface area of air-cathode used in MFC and Zn-air battery was ca. 12.56 cm^2 (4.0 cm diameter) and 12 cm^2 (3 cm × 4 cm), respectively.

S6. Operation of MFC and Zn-air battery. The MFCs were inoculated with anaerobic sludge collected from Xiajiahe municipal wastewater treatment plant

(Dalian, China). The anodic medium contained glucose (COD=890 mg L^{-1}), 130 mg L^{-1} KCl, 310 mg L^{-1} NH_4Cl, 50 mmol L^{-1} phosphate buffer nutrient solution (PBS, mixture of Na_2HPO_4 and NaH_2PO_4, pH 7.13), 12.5 ml L^{-1} trace minerals, and 5 mL L^{-1} vitamins, which was periodically refreshed when the voltage dropped below 20 mV. The cell voltage was monitored using a 32-channel PISO-813/S (ICP DAS, Taiwan) online data logging system at a recording interval of 10 minutes. The polarization and power density curves of MFC were obtained by varying the external resistance in descending order starting from the open-circuit, followed by a range from 10 KΩ to 10 Ω when the voltage output achieved a steady state. The anode potential variations were determined with an Ag/AgCl inserted into the anode chamber. The power density was normalized to the projected cathode surface area.

The measurements of the Zn-air battery were performed using home-built electrochemical cells. Zinc foil was used as the anode. The discharge curves of the Zn-air battery was recorded at a current density of 10 mA cm^{-2} using the Fe-N-C/800-HT2 or Pt/C E-TEK (20 wt%) based air-cathode in O_2-saturated 6 mol L^{-1} KOH + 0.2 mol L^{-1} zinc acetate ($Zn(Ac)_2$) electrolyte. Polarization curves and galvanostatic discharge curves were collected by a CHI 760D electrochemical workstation (CH Instruments, China) at room temperature.

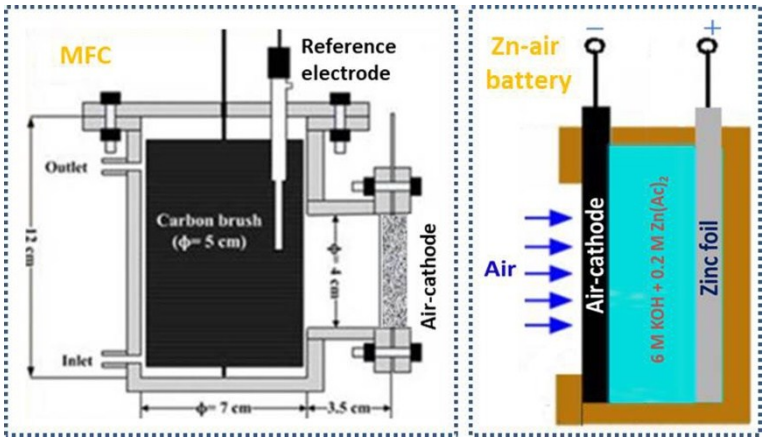

Figure S1 The structure diagrams of single-chamber air-cathode MFC and primary zinc-air battery.

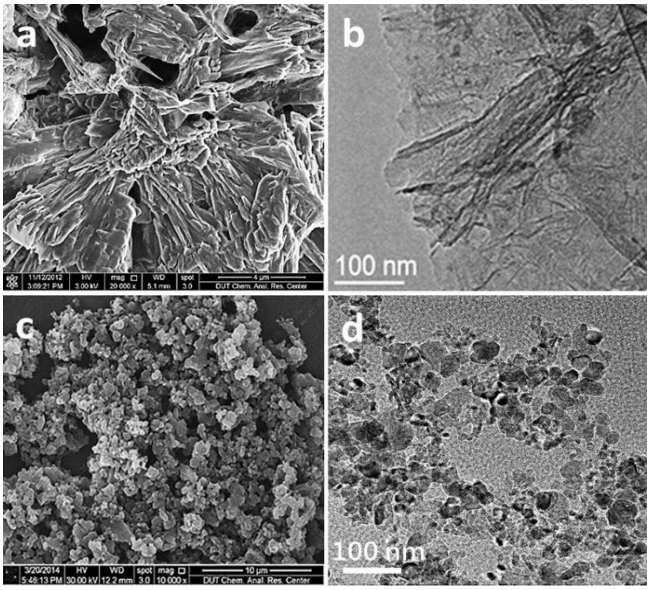

Figure S2 SEM images of c-PDAA/800-HT1 **(a)** and c-PB/800-HT1 **(c)**, TEM images of c-PDAA/800-HT1 **(b)** and c-PB/800-HT1 **(d)**.

In 0.1 mol L^{-1} KOH	In 0.1 mol L^{-1} PBS
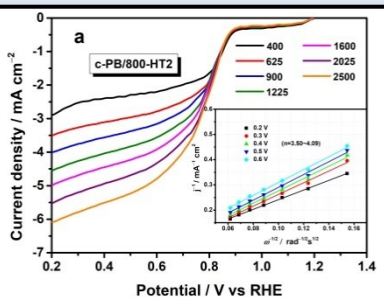	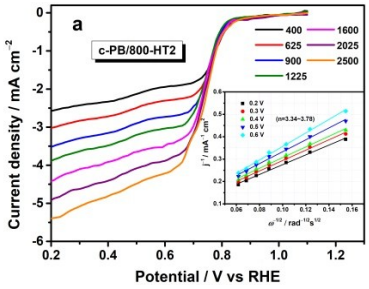
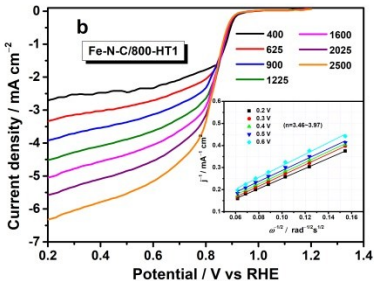	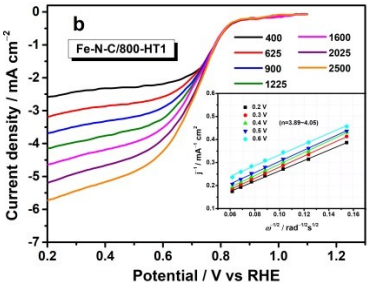
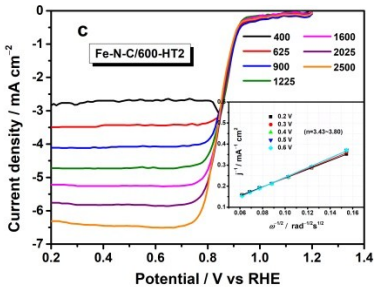	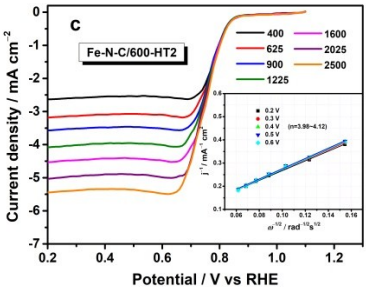
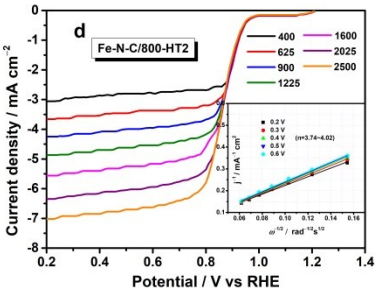	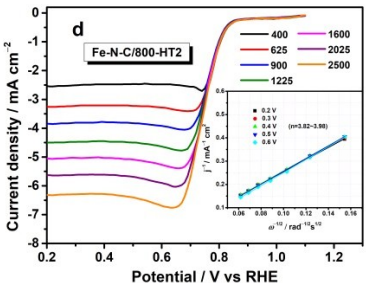
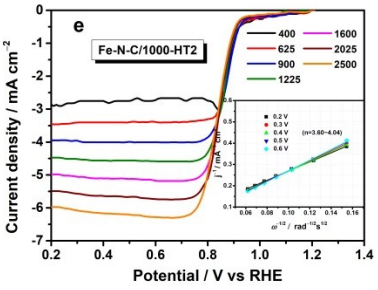	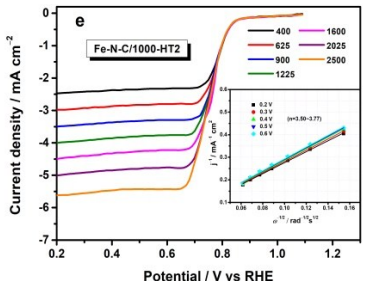
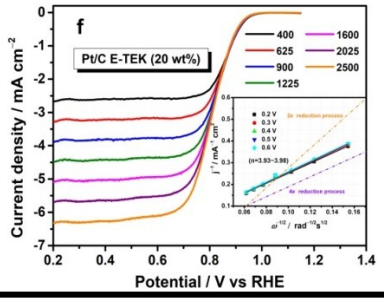	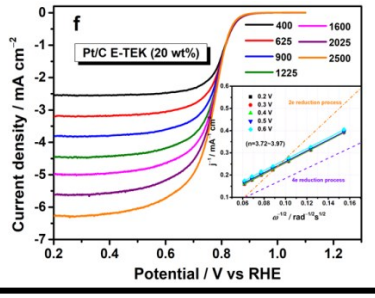

Figure S3 RDE polarization curves of different catalysts in O_2-saturated 0.1 mol L^{-1} KOH (left column) and 0.1 mol L^{-1} PBS (right column) solutions at different rotating speeds with a scan rate of 10 mV s^{-1}. The insets show the corresponding K-L plots at different potentials from 0.2 V to 0.6 V.

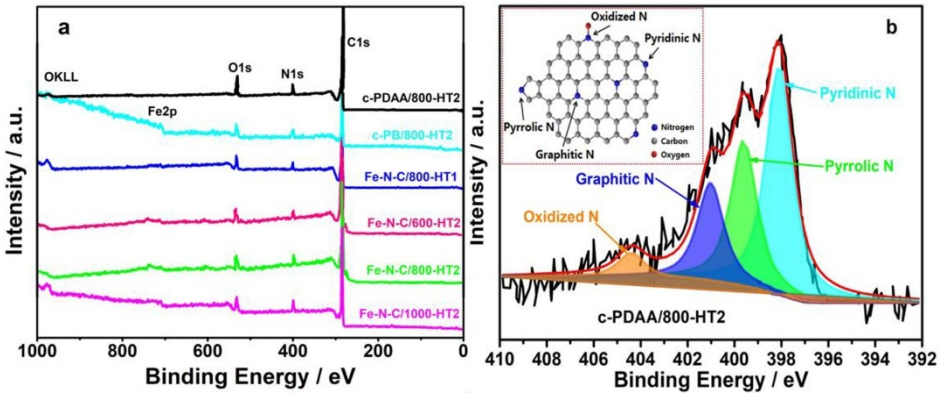

Figure S4 XPS survey spectra of the different catalysts **(a)** and high-resolution N 1s spectrum of c-PDAA/800-HT2 sample **(b)**.

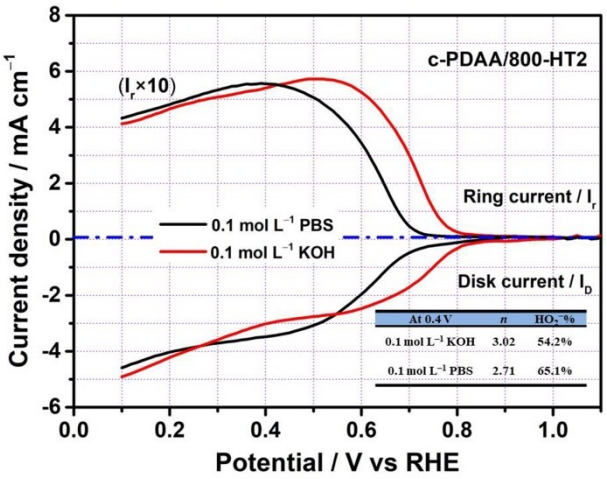

Figure S5 RRDE voltammetry curves of c-PDAA/800-HT2 recorded at a scan rate of 10 mV s^{-1} and a rotating speed of 1600 rpm in O_2-saturated 0.1 mol L^{-1} KOH and PBS solutions. The inset table shows the corresponding values of *n* and HO_2^-% obtained at 0.4 V vs RHE.

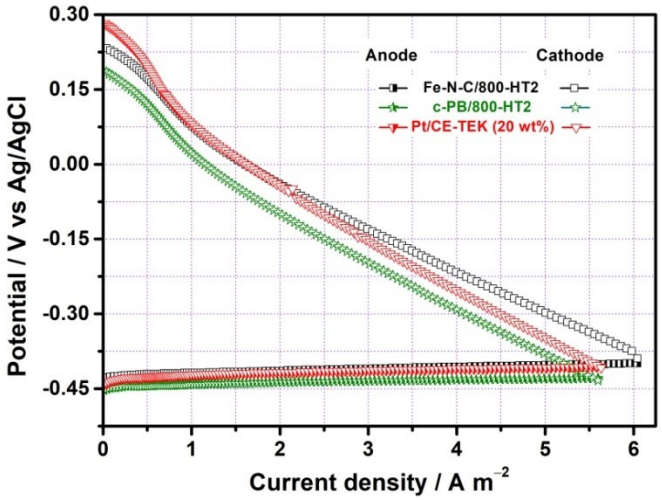

Figure S6 Cathode and anode potential (vs. Ag/AgCl) polarization curves of single-charmer air-cathode MFCs assembled with different cathodic catalysts.

Table S1 The BET surface area, pore volume, and average pore size of all the prepared samples.

Materials	BET surface area (m^2 g^{-1})	Pore volume / (cm^3 g^{-1})	Average pore size (nm)
c-PDAA/800-HT2	662.08	0.44	6.15
c-PB/800-HT2	227.27	0.16	6.64
Fe-N-C/800-HT1	380.45	0.22	7.45
Fe-N-C/600-HT2	514.72	0.32	5.36
Fe-N-C/800-HT2	617.43	0.35	5.12
Fe-N-C/1000-HT2	463.18	0.30	5.87

Table S2 Summary of surface chemical states and atom percentage of different N species in each catalyst determined from high-resolution N1s XPS analysis.

Components	Quantity /at.%					
	c-PDAA/800-HT2	c-PB/800-HT2	Fe-N-C/800-HT1	Fe-N-C/600-HT2	Fe-N-C/800-HT2	Fe-N-C/1000-HT2
Pyridinic N	1.33	0.86	1.23	0.90	0.82	0.70
Fe-N_x	-	0.88	0.92	1.07	1.12	0.84
Pyrrolic N	1.36	1.12	1.21	0.93	0.83	0.96
Graphitic N	1.74	1.06	1.26	0.97	1.06	0.92
Oxidized N	0.78	0.57	0.81	0.82	0.54	0.44
Total doped N	5.21	4.49	5.43	4.69	4.37	3.86

Table S3 Comparison of ORR performance in alkaline and neutral medium of Fe-N-C/800-HT2 with literature values.

Materials	Electrolyte	Catalyst loading (mg cm^{-2})	E_{onset} (V vs. RHE)	$E_{1/2}$ (V vs. RHE)	Ref.
Fe-N-C/800-HT2	0.1 M KOH (1600 rpm)	**0.31**	**1.01**	**0.881**	**This work**
Fe-N-CNBs-600		0.429	1.030	0.875	4
Fe-N-C-800		0.459	N/A	0.883	5
Fe/N/S-CNTs		1.0	0.987	0.887	6
Fe-N/C-800		0.1	0.923	0.809	7
Fe-N-CNFs		0.6	0.930	0.81	8
Fe/Fe_3C@C/RGO		0.556	1.00	0.93	9
Fe_3C/NG-800		0.4	1.03	0.86	10
Fe/N/S-PCNT		0.1	0.96	0.84	11
Fe/NS/C-g-C_3N_4/TPTZ		0.4	1.0	0.868	12
Fe,N/PGC-30		0.34	0.96	0.82	13
3D Fe-N-C		0.5	N/A	0.88	14
C-2PANI/PBA		0.36/0.28	N/A	0.85	15
N-doped Fe-Fe_3C@C		0.7	-0.05 (Ag/AgCl)	N/A	16
Fe-NMP		0.4	0.97	0.84	17
ICM-FePhen3		0.8	N/A	0.86	18
Fe@BC-800		0.42	1.01	0.85	19
Fe-N/C-1/30		ca. 0.41	1.04	0.895	20
Fe–N–C PCSs		0.255	1.03	0.84	21
Fe/Fe_2O_3@Fe-N-C-1000		ca. 0.6	-0.04 (Ag/AgCl)	-0.17 (Ag/AgCl)	22
Fe-N-C/800-HT2	0.1 M PBS (1600 rpm)	**0.31**	**0.862**	**0.743**	**This work**
Fe,N/PGC-30		0.34	0.85	0.61	13
Fe-N-G		0.5	0.22 (SCE)	N/A	23
3D Fe-N-C		0.5	0.23 (SCE)	-0.08 (SCE)	24
Fe@BC-800		0.42	0.86	0.68	19
N-Fe/Fe_3C@C		0.5	>0.21 (Ag/AgCl)	N/A	25
Fe-N-C (Ricobendazole)		2 ± 0.1	0.235 (Ag/AgCl)	N/A	26

Table S4 Comparison of the Zn-air battery performance of Fe-N-C/800-HT2 with literature values.

Materials	Peak power density (mW cm^{-2})	Open-circuit potential (V)	Ref.
Fe-N-C/800-HT2	**246.4**	**1.424**	**This work**
Fe-N-C-800	135.3	1.476	5
Fe/N/S-CNTs	111	1.49	6
Fe–N-CNBs-600	257	1.53	4
Fe-N/C-1/30	121.8	1.525	20
Fe@C-NG/NCNTs	101.3	1.373	27
S,N-Fe/N/C-CNT	102.7	1.35	28
FeNC-1000	55	1.42	29
Fe/Co-N/S-C	102.63	1.395	30
Fe/Fe_2O_3@Fe-N-C-1000	193	1.47	22
Fe/NS/C-g-C_3N_4/TPTZ	225	1.385	12

Reference

1 X. Li, H. Li, M.-R. Huang, *Chem. Eur. J*., 2007, **13**, 8884.

2 W. Gu, L. Hu, J. Li, E. Wang, *J. Mater. Chem. A*, 2016, **4**, 14364.

3 X. Ma, Z. Lei, W. Feng, Y. Ye, C. Feng, *Carbon*, 2017, **123**, 481.

4 L. Cao, Z. Li, Y. Gu, D. Li, K. Su, D. Yang, B. Cheng, *J. Mater. Chem. A*, 2017, **5**, 11340.

5 D. Wang, L. Xiao, P. Yang, Z. Xu, X. Lu, L. Du, O. Levin, L. Ge, X. Pan, J. Zhang, M. An, *J. Mater. Chem*. *A*, 2019, **7**, 11007.

6 H. Jin, H. Zhou, W. Li, Z. Wang, J. Yang, Y. Xiong, D. He, L. Chen, S. Mu, *J. Mater. Chem. A,* 2018, **6**, 20093.

7 L. Lin, Q. Zhu, A. Xu, *J. Am. Chem. Soc*., 2014, **136**, 11027.

8 Z. Wu, X. Xu, B. Hu, H. Liang, Y. Lin, L. Chen, S. Yu, *Angew. Chem. Int. Ed*., 2015, **54**, 8179.

9 Y. Hou, T. Huang, Z. Wen, S. Mao, S. Cui and J. Chen, *Adv. Energy Mater.*, 2014, **4**, 1220.

10 M. Xiao, J. Zhu, L. Feng, C. Liu and W. Xing, *Adv. Mater*., 2015, **27**, 2521.

11 Z. Tan, H. Li, Q. Feng, L. Jiang, H. Pan, Z. Huang, Q. Zhou, H. Zhou, S. Ma, Y. Kuang, *J. Mater. Chem. A*, 2019, **7**, 1607.

12 X. Liu, C. Chen, Q. Cheng, L. Zou, Z. Zou, H. Yang, *Catalysts*, 2018, **8**, 158.

13 W. Gu, L. Hu, J. Li, E. Wang, *J. Mater. Chem. A*, 2016, 4, 14364.

14 W. Wang, W. Chen, P. Miao, J. Luo, Z. Wei, S. Chen, *ACS Catal*., 2017, **7**, 6144.

15 X. Wang, L. Zou, H. Fu, Y. Xiong, Z. Tao, J. Zheng, X. Li, *ACS Appl. Mater. Interfaces*, 2016, **8**, 8436.

16 B.K. Barman, K.K. Nanda, *Green Chem*., 2016, **18**, 427.

17 M. M. Hossen, K. Artyushkova, P. Atanassov, A. Serov, *J. Power Sources*, 2018, **375**, 214.

18 J. Li, Q. Jia, S. Mukerjee, M.-T. Sougrati, G. Drazic, A. Zitolo, F. Jaouen, *Catalysts*, 2019, **9**, 144.

19 X. Ma, Z. Lei, W. Feng, Y. Ye, C. Feng, *Carbon*, 2017, **123**, 481.

20 W. Wei, X. Shi, P. Gao, S. Wang, W. Hu, X. Zhao, Y. Ni, X. Xu, Y. Xu, W. Yan,

H. Ji, M. Cao, *Nano Energy*, 2018, **52**, 29.
21 J.-T. Ren, Z.-Y. Yuan, *J. Mater. Chem. A*, 2019, **7**, 13591.
22 Y. Zang, H. Zhang, X. Zhang, R. Liu, S. Liu, G. Wang, Y. Zhang, H. Zhao, *Nano Res*., 2016, **9**, 2123.
23 S. Li, Y. Hu, Q. Xu, J. Sun, B. Hou, Y. Zhang, *J. Power Source*, 2012, **213**, 265.
24 H. Tang, Y. Zeng, Y. Zeng, R. Wang, S. Cai, C. Liao, H. Caia, X. Lu, P. Tsiakarasc, *Appl. Catal. B*, 2017, **202**, 550.
25 Z. Wen, S. Ci, F. Zhang, X. Feng, S. Cui, S. Mao, S. Luo, Z. He, J. Chen, *Adv. Mater.*, 2012, **24**, 1399.
26 C. Santoro, A. Serov, R. Gokhale, S. Rojas-Carbonell, L. Stariha, J. Gordon, K. Artyushkova, P. Atanassov, *Appl. Catal. B*, 2017, **205**, 24.
27 Q. Wang, Y. Lei, Z. Chen, N. Wu, Y. Wang, B. Wang and Y. Wang, *J. Mater. Chem. A*, 2018, **6**, 516.
28 P. Chen, T. Zhou, L. Xing, K. Xu, Y. Tong, H. Xie, L. Zhang, W. Yan, W. Chu, C. Wu and Y. Xie, *Angew. Chem. Int. Ed.*, 2017, **56**, 610.
29 G. Ren, L. Gao, C. Teng, Y. Li, H. Yang, J. Shui, X. Lu, Y. Zhu and L. Dai, *ACS Appl. Mater. Inter.*, 2018, **10**, 10778.
30 Y. Zhao, Q. Lai, Y. Wang, J. Zhu and Y. Liang, *ACS Appl. Mater. Inter*., 2017, **9**, 16178.